Conjugated Polymers of Fused Bithiophenes with Enhanced π-Electron Delocalization for Photovoltaic Applications

ARTICLE *in* MACROMOLECULES · AUGUST 2008

Impact Factor: 5.8 · DOI: 10.1021/ma800776q

3 AUTHORS:

Shengqiang Xiao
Wuhan University of Technology
49 PUBLICATIONS **1,516** CITATIONS
SEE PROFILE

Huaxing Zhou
University of North Carolina at Chapel Hill
26 PUBLICATIONS **3,326** CITATIONS
SEE PROFILE

Wei You
University of North Carolina at Chapel Hill
81 PUBLICATIONS **4,339** CITATIONS
SEE PROFILE

Conjugated Polymers of Fused Bithiophenes with Enhanced π-Electron Delocalization for Photovoltaic Applications

Shengqiang Xiao, Huaxing Zhou, and Wei You*

Department of Chemistry, University of North Carolina at Chapel Hill, Chapel Hill, North Carolina 27599-3290

Received April 7, 2008; Revised Manuscript Received May 31, 2008

ABSTRACT: We designed and synthesized a family of three structurally related conjugated alternating copolymers, namely poly[2,6-(4,4-dioctyl-4*H*-cyclopenta[2,1-*b*:3,4-*b*]dithiophene)-*alt*-2,7-(4,5-dioctylbenzo[2,1-*b*:3,4-*b*′]dithiophene)] (**PBDT**), poly[2,6-(4,4-dioctyl-4*H*-cyclopenta[2,1-*b*:3,4-*b*′]dithiophene)-*alt*-2,9-(5,6-dioctylnaphtho[2,1-*b*:3,4-*b*′]dithiophene)] (**PNDT**), and poly[2,6-(4,4-dioctyl-4*H*-cyclopenta[2,1-*b*:3,4-*b*′]dithiophene)-*alt*-6,9-(2,3-bis((*S*)-2,6-dimethylheptyl)dithieno[3,2-*f*:2′,3′-*h*]quinoxaline] (**PQDT**). The repeating units of these three copolymers consist of two modified bithiophene units with one of them planarized by bridging benzo, naphtho, and quinoxalino segments, respectively. The 2,6-(4,4-dioctyl-4*H*-cyclopenta)[2,1-*b*;3,4-*b*′]dithiophene moieties were introduced as the other bithiophene unit to improve the solubility of resultant copolymers, facilitating the polymers characterization and photovoltaic devices fabrications. All polymers were fully characterized, and their applications as donor materials in conjunction with PCBM as acceptor in bulk heterojunction (BHJ) photovoltaic devices were tested. The increased conjugation from naphtha and quinoxalino segments over benzo unit led to the decreased band gap of **PNDT** and **PQDT** compared to that of **PBDT**. A lower HOMO level was observed from **PQDT** due to the presence of two nitrogen atoms in the planarized π system, which rendered the conjugated molecule electron-deficient. BHJ photovoltaic devices made from **PQDT**:PCBM film (1:1.6, 100 nm) exhibited a V_{oc} value of 0.53 V, a J_{sc} value of 4.56 mA/cm^2, and a *FF* of 0.47, offering an overall power conversion efficiency of 1.14% and a peak quantum efficiency of 37% from IPCE measurement. The best performance of **PQDT** among three polymer investigated was correlated with its lower optical band gap (1.96 eV), lower HOMO level (−5.15 eV), and higher hole mobility (5.15×10^{-5} cm^2 V^{-1} s^{-1}). We concluded that the intrinsic electronic properties of these planarized bithiophene moieties offered moderate flexibility in fine-tuning electronic properties of the corresponding copolymers.

Introduction

Tremendous research efforts have been devoted to the development of polymer-based organic photovoltaic (OPV) cells during the past two decades due to projected advantages of these solar cells over their inorganic counterparts, including flexibility, facile processing and manipulation, low weight, and low cost. The mechanism by which light is converted into electricity in these OPV devices consists of the following fundamental steps: light absorption, exciton generation, exciton migration, exciton dissociation, and charge transport. The bulk heterojunction (BHJ) of regioregular poly(3-hexylthiophene) (RR-P3HT) and [6,6]-phenyl C_{61}-butyric acid methyl ester (PCBM) represents one of the most successful systems with reproducible efficiencies approaching 5% after careful optimization.[1,2] To further improve the performance of polymer-based BHJs, one has to carefully address the following issues. First, the HOMO and LUMO energy levels of the donor and acceptor components need to have optimal offset to maximize the attainable open circuit voltage (V_{oc}). Second, the active layer should have compatible absorption with respect to the solar spectrum to maximize the efficiencies of exciton generation, which sets the upper limit for the short-circuit current J_{sc}. Finally, the morphology of the active layer, which governs the physical interaction between the donor and the acceptor, should be optimized to promote charge separation and favorable transport of photogenerated charges and to maximize the attainable J_{sc} and fill factor (*FF*).[3,4]

Fulfilling these requirements presents serious challenges in the design of new semiconductive conjugated polymers to be employed as active donors in polymer-based BHJ photovoltaic devices. For example, a number of low band gap polymers have been developed in recent years in the attempt to increase the device efficiency by improving light harvesting.[5−15] However, none of them can outperform P3HT in terms of energy conversion efficiency, mainly due to high-lying HOMO energy level with regard to the LUMO of the acceptor (usually PCBM), which reduces the V_{oc}, or ill-defined morphology of the active blend, which reduces the J_{sc} and *FF* (or both). In our search for new donor materials, polycyclic aromatic moieties drew our attention. Their rigidly enforced planarity would benefit more effective π-electron delocalization when incorporated into the conjugated polymer backbone, which would lead to decreased optical band gaps while providing $\pi-\pi$ interactions between polymer chains in thin solid films, thereby improving charge carrier mobility in devices.[16−21]

To exemplify the application of the unique features associated with these polycyclic aromatic moieties for polymer-based photovoltaics, we synthesized a family of three structurally related conjugated alternating copolymers, namely poly[2,6-(4,4-dioctyl-4*H*-cyclopenta[2,1-*b*:3,4-*b*]dithiophene)-*alt*-2,7-(4,5-dioctylbenzo[2,1-*b*:3,4-*b*′]dithiophene)] (**PBDT**), poly[2,6-(4,4-dioctyl-4*H*-cyclopenta[2,1-*b*:3,4-*b*]dithiophene)-*alt*-2,9-(5,6-dioctylnaphtho[2,1-*b*:3,4-*b*′]dithiophene)] (**PNDT**), and poly[2,6-(4,4-dioctyl-4*H*-cyclopenta[2,1-*b*:3,4-*b*′]dithiophene)-*alt*-6,9-(2,3-bis((*S*)-2,6-dimethylheptyl)dithieno[3,2-*f*:2′,3′-*h*]quinoxaline] (**PQDT**) (Figure 1). The repeating units of these three copolymers consist of two modified bithiophene units with one of them planarized by bridging benzo, naphtho, and quinoxalino segment, respectively. The known 2,6-(4,4-dioctyl-4*H*-cyclopenta)[2,1-*b*;3,4-*b*′]dithiophene moieties were introduced as the other bithiophene unit to improve the solubility of resultant copolymers, facilitating polymer characterization and photovoltaic devices fabrications. The intrinsic electronic properties

* To whom all correspondence should be addressed. E-mail: wyou@email.unc.edu.

10.1021/ma800776q CCC: $40.75
Published on Web 07/12/2008

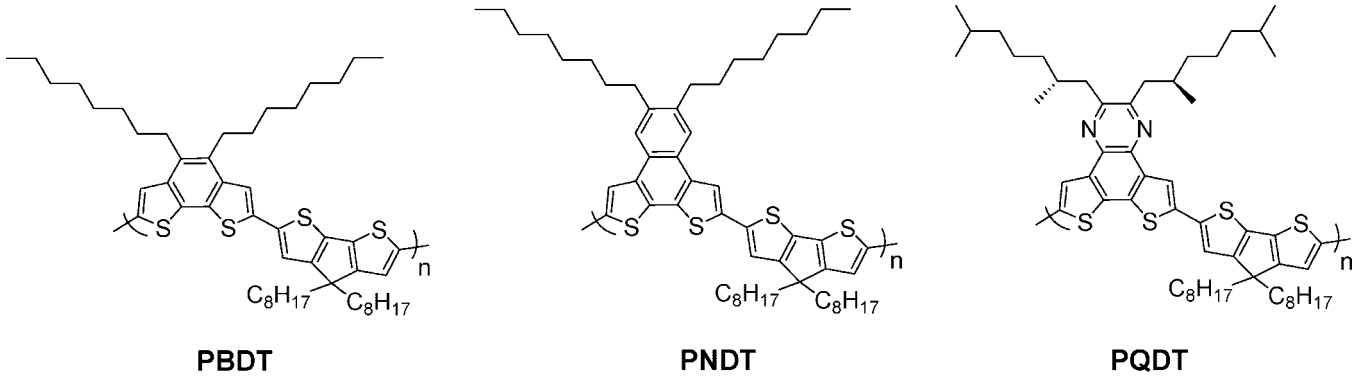

Figure 1. Structures of three alternating copolymers **PBDT**, **PNDT**, and **PQDT**.

Scheme 1. Synthesis of Copolymer PQDT[a]

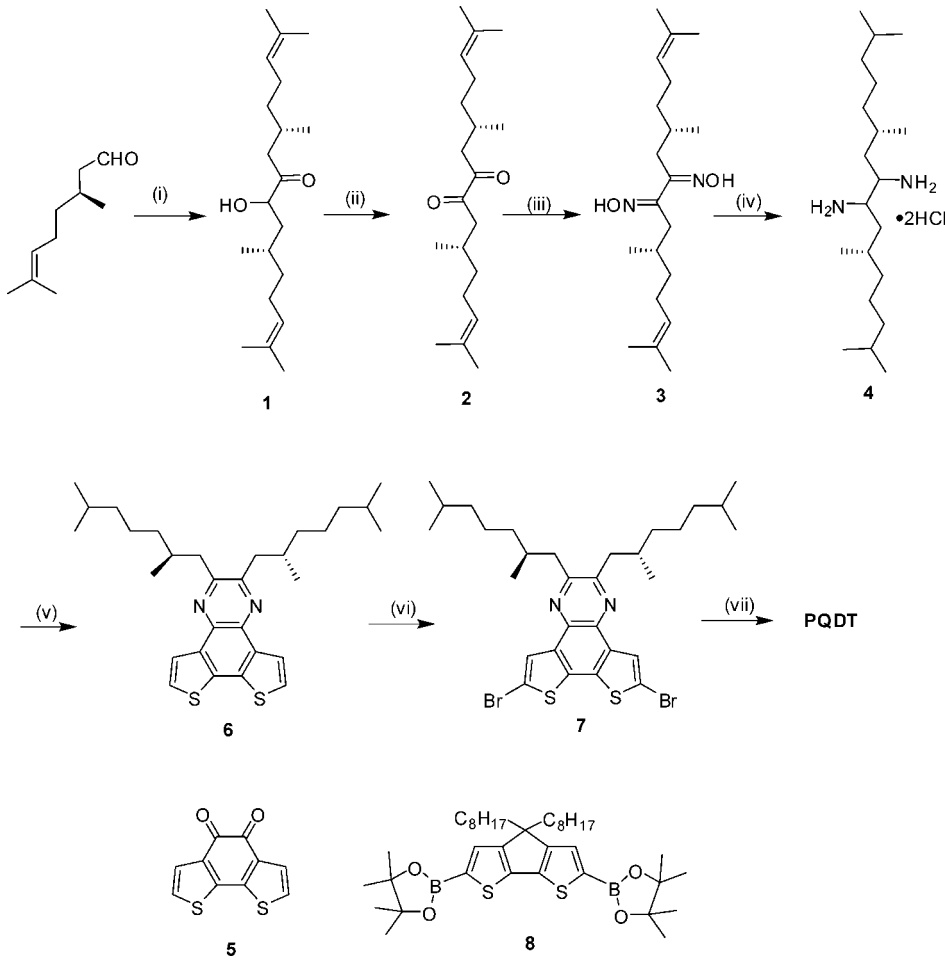

[a] Reagents and conditions: (i) 3-ethyl-5-(2-hydroxyethyl)-4-methylthiazolium bromide, triethylamine, ethanol, Ar, reflux overnight; (ii) pyridinium chlororchromate (PCC), methylene chloride, reflux overnight; (iii) hydroxyammonium chloride, pyridine, ethanol, reflux for 5 h; (iv) platinum oxide, H_2, concentrated hydrogen chloride, absolute ethanol, rt; (v) **5**, pyridine, methanol, reflux overnight; (vi) NBS, $CHCl_3$−HOAc (1:1, v/v), rt; (vii) **8**, tetrakis(triphenylphosphine)palladium, Na_2CO_3, toluene, H_2O, reflux, 7 days.

of these planarized bithiophene moieties offered moderate flexibility in fine-tuning electronic properties of the corresponding copolymers. In this paper, we present the synthesis, the physical properties, and the preliminary photovoltaic performances of these structurally related copolymers. The elucidated structure/property relationships will assist the intelligent exploration of future design of materials for OPV applications.

Results and Discussion

Monomer Synthesis. To obtain benzo[2,1-*b*:3,4-*b*′]dithiophene, naphtho[2,1-*b*:3,4-*b*′]dithiophene, and quinoxalino[2,1-*b*:3,4-*b*′]dithiophene moieties for the preparation of polymers **PBDT**, **PNDT**, and **PQDT**, different synthetic strategies were applied to bridge various π systems to the bithiophene unit. Side alkyl chains were incorporated to improve solubility of resulting polymers. The synthetic route for the preparation of dibrominated monomer quinoxalino[2,1-*b*:3,4-*b*′]dithiophene (**7**) for **PQDT** is shown in Scheme 1. Quinoxalino[2,1-*b*:3,4-*b*′]dithiophene was achieved via the condensation reaction of an alkylated vicinal diamine **4** with 1,2-diketone of benzo[2,1-*b*:3,4-*b*′]bithiophene-4,5-quinone (**5**). 1,2-Diamine **4** was obtained through multistep synthesis from commercially available

Scheme 2. Synthesis of Copolymer PBDT[a]

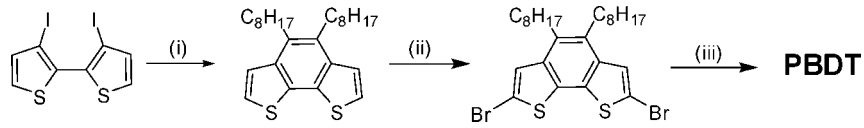

[a] Reagents and conditions: (i) palladium acetate, 9-octadecyne, tributylamine, anhydrous DMF, 130°C; (ii) NBS, $CHCl_3$−HOAc (1:1, v/v), rt; (iii) **8**, tetrakis(triphenylphosphine)palladium, Na_2CO_3, toluene, H_2O, reflux, 7 days.

Scheme 3. Synthesis of Copolymer PNDT[a]

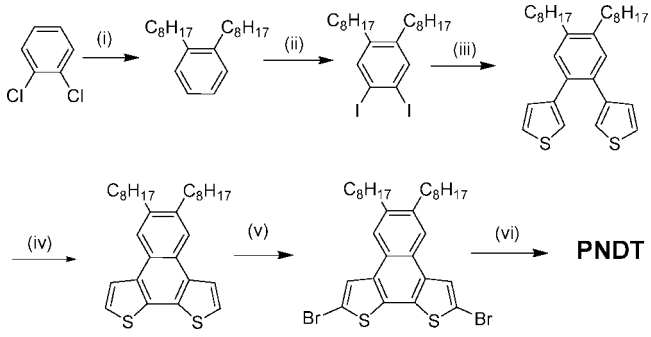

[a] Reagents and conditions: (i) octylmagnesium bromide, 1,3-bis(diphenylphosphino)propane)nickel(II) chloride, anhydrous ethyl ether; (ii) I_2, $NaIO_3$ HOAc−H_2SO_4−H_2O, reflux; (iii) 3-thiopheneboronic acid, $Pd(PPh_3)_4$, Na_2CO_3, toluene, EtOH and H_2O, reflux; (iv) I_2, O_2, under irradiation of 400 W mercury lamp; (v) NBS, $CHCl_3$−HOAc (1:1, v/v), rt; (vi) **8**, tetrakis(triphenylphosphine)palladium, Na_2CO_3, toluene, H_2O, reflux, 7 days.

aldehyde **1**. The classical acyloin condensation of aldehyde **1** followed by PCC oxidation gave alkylated 1,2-diketone **2**, which was converted to 1,2-dioxime **3** and followed by Pt-catalyzed hydrogenation to give the hydrogen chloride salt of 1,2-diamine in almost quantitative yield. The condensation of 1,2-diamine **4** with 1,2-diketone benzo[2,1-*b*:3,4-*b*′]bithiophene-4,5-quinone (**5**) under aerobic conditions directly afforded the dehydrogenated product of quinoxalino[2,1-*b*:3,4-*b*′]dithiophene (**6**). Dibromination of **6** was accomplished using *N*-bromosuccinimide (NBS) to provide final comonomer **7**. The other comonomer **8** was prepared by dilithiation of 4,4-dioctyl-4*H*-cyclopenta[2,1-*b*:3,4-*b*′]dithiophene using *n*-BuLi followed by quenching the intermediate with 2-isopropoxy-4,4,5,5-tetramethyl[1,3,2]dioxaborolane.

The preparation of 2,7-dibromo-4,5-dioctylbenzo[2,1-*b*:3,4-*b*′]dithiophene is depicted in Scheme 2. The synthesis was completed by a palladium-catalyzed coupling reaction between 3,3′-diiodo-2,2′-bithiophene and 9-octadecyne[22,23] followed by NBS bromination in a mixed solvent of chloroform/acetic acid.

As outlined in Scheme 3, the preparation of 2,9-dibromo-5,6-dioctylnaphtho[2,1-*b*:3,4-*b*′]dithiophene started from 1,2-dichlorobenzene. A nickel-catalyzed Kumada coupling reaction between 1,2-dichlorobenzene and freshly prepared octylmagnesium bromide offered 1,2-dioctylbenzene. Iodination of 1,2-dioctylbenzene followed by palladium-catalyzed Suzuki coupling reaction with 3-thiopheneboronic acid provided 4,5-bis(3-thienyl)-1,2-dioctylbenzene at high yield.[18] 5,6-Dioctylnaphtho[2,1-*b*:3,4-*b*′]dithiophene was then prepared via oxidative photocyclization by irradiation of a diluted toluene solution of 4,5-bis(3-thienyl)-1,2-dioctylbenzene under ambient conditions in the presence of a catalytic amount of iodine.[24,25] Subsequent bromination using NBS in a mixed solvent of chloroform/acetic acid offered the comonomer 2,9-dibromo-5,6-dioctylnaphtho[2,1-*b*:3,4-*b*′]dithiophene.

Polymer Synthesis. All copolymers were synthesized by a polycondensation of 2,6-bis(4,4,5,5-tetramethyl-1,3,2-dioxaborolan-2-yl)-4,4-dioctyl-4*H*-cyclopenta[2,1-*b*:3,4-*b*′]dithiophene (**8**) and corresponding dibrominated comonomers through Suzuki coupling reactions. All crude copolymers were washed successively by water and methanol and extracted by methanol and acetone successively using a Soxhlet apparatus to remove byproducts and oligomers. Finally, the polymers were extracted by chloroform, recollected by precipitating them into methanol, and dried under vacuum. The alternating copolymers **PBDT**, **PNDT**, and **PQDT** are soluble in common organic solvents such as methylene chloride, chloroform, THF, and toluene and can be easily processed into thin films for further characterizations. The molecular structures of all alternating copolymers were confirmed by ^{1}H NMR spectroscopy (Supporting Information).

Table 1. Polymerization Results for Polymers PBDT, PNDT, and PQDT

	yield[a] [%]	M_w[b] [kg/mol]	M_n[b] [kg/mol]	PDI[b]	T_d[c] [°C]
PBDT	88	39.1	20.6	1.90	432
PNDT	90	25.8	16.6	1.54	432
PQDT	86	30.9	16.1	1.91	430

[a] Soluble polymers extracted by $CHCl_3$ with respect to the overall yield. [b] Determined by GPC in THF using polystyrene standards. [c] The temperature of degradation corresponding to a 5% weight loss determined by TGA at a heating rate of 10 °C/min.

The yields and molecular weights of three copolymers are listed in Table 1. High polymer yields (∼90%) were obtained from Suzuki coupling polymerizations. The molecular weights were determined by gel permeation chromatography (GPC) in THF using polystyrene standards. Thermogravimetric analysis (TGA) and differential scanning calorimetry (DSC) analysis revealed that all polymers did not degrade below 430 °C nor did they melt (Supporting Information).

Optical Absorption. The electronic absorption data of the three alternating copolymers are listed in Table 2. All spectroscopic properties were measured both in toluene solutions (Figure 2a) and as thin films on glass slides (Figure 2b). As shown in Figure 2a, **PNDT** and **PQDT** have almost identical absorption maxima at 552 nm, which is 15 nm red-shifted compared to that of **PBDT**. The low energetic edge of the absorption spectrum of individual polymer was used to approximate the band gap of corresponding polymer. The band gap of **PBDT** was estimated to be 2.06 eV (absorption edge: ∼600 nm), while a smaller band gap of 1.96 eV was calculated for **PNDT** and **PQDT** (absorption edge: ∼631 nm). Such a decrease in the band gap can be explained by the fact that the naphthalene and quinoxalene units provide more conjugation than the benzene unit when incorporated into the bithiophene unit in the conjugated backbone of copolymers. A similar behavior was observed for the absorption spectra of the three polymers at thin films (Figure 2b). Unexpectedly, only a tiny red shift (less than 5 nm) was observed for the absorptions from solution to thin film for all copolymers, which suggests less interchain stacking induced by $\pi-\pi$ interaction.[16] The negligible absorption shift between solution and thin film of three copolymers may be caused by the two octyl groups in 4*H*-cyclopenta[2,1-*b*:3,4-*b*′]-dithiophene moiety, which imparts steric hindrance and affects the planarity of the conjugated backbone.

Table 2. Optical and Electrochemical Data of the Polymers PBDT, PNDT, and PQDT

	UV−vis absorption data								
	toluene solution			film			cyclic voltammetry		
polymer	λ_{max} [nm]	λ_{onset} [nm]	E_g[a] [eV]	λ_{max} [nm]	λ_{onset} [nm]	E_g[a] [eV]	E^{ox}_{onest} HOMO [V/eV]	E^{red}_{onest} LUMO [V/eV]	E^{EC}_{gap} [eV]
PBDT	538	602	2.06	538	617	2.00	0.24/−5.04	−1.97/−2.83	2.21
PNDT	552	631	1.96	555	650	1.91	0.24/−5.04	−1.86/−2.94	2.10
PQDT	554	631	1.96	555	641	1.94	0.35/−5.15	−1.75/−3.05	2.10

[a] Calculated from the intersection of the tangent on the low energetic edge of the absorption spectrum with the abscissa.

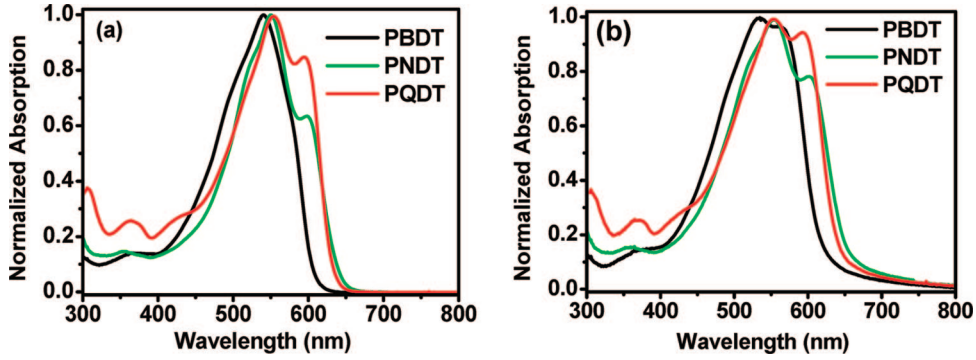

Figure 2. Normalized UV−vis absorption spectra of **PBDT**, **PNDT**, and **PQDT** (a) in toluene solution and (b) as thin films.

Electrochemistry. Cyclic voltammetry (CV) was employed to investigate the electrochemical properties of the three copolymers and to determine the energy levels of individual copolymers. Cyclic voltammograms of the oxidation and reduction behaviors (Supporting Information) were recorded from thin films of **PBDT**, **PNDT**, and **PQDT** drop-casted from chloroform solutions as described in the Experimental Section. The potentials were internally calibrated using the ferrocene/ferrocenium redox couple (Fc/Fc^+), which has a known reduction potential of 4.8 eV.[26,27] The highest occupied molecular orbital (HOMO) and lowest unoccupied molecular orbital (LUMO) energy levels of copolymers were calculated from the onset oxidation potentials (E^{ox}_{onset}) and onset reductive potentials (E^{red}_{onset}), respectively, according to eqs 1 and 2. The electrochemically determined band gaps were deduced from the difference between onset potentials from oxidation and reduction of copolymers as depicted in eq 3.

$$\text{HOMO} = -(E^{ox}_{onset} + 4.8)\ \text{(eV)} \quad (1)$$

$$\text{LUMO} = -(E^{ox}_{onset} + 4.8)\ \text{(eV)} \quad (2)$$

$$E^{EC}_{gap} = E^{ox}_{onset} - E^{red}_{onset} \quad (3)$$

The CV data of three copolymers are presented in Table 2. The band gap of **PNDT** or **PQDT** with bridged naphtho or quinoxalino segment to bithiophene moiety showed a decrease of ca. 0.1 eV compared to that of **PBDT** with bridged benzo segment. This behavior is consistent with the results from UV−vis absorption spectra. However, the HOMO energy level of **PNDT** remained unchanged as compared to that of **PBDT** (−5.04 eV). Compared with **PBDT** and **PNDT**, **PQDT** showed a decrease of ca. 0.1 eV in its HOMO energy level (−5.15 eV). The LUMO energy level of **PQDT** also decreased about 0.1 eV accordingly to maintain a band gap of 2.10 eV. The noticeably lower HOMO and LUMO levels in the case of **PQDT** are ascribed to the two nitrogen atoms in the planarized π system because these two nitrogen atoms render the resulting conjugated molecule more electron-deficient. From these results, we conclude that bridging different π segments with intrinsically different electronic properties to the bithiophene moieties allows a moderate modulation of the band gap and energy level of resulting polymers. This finding will assist future design of semiconductive polymers with tunable electronic properties toward OPV applications.

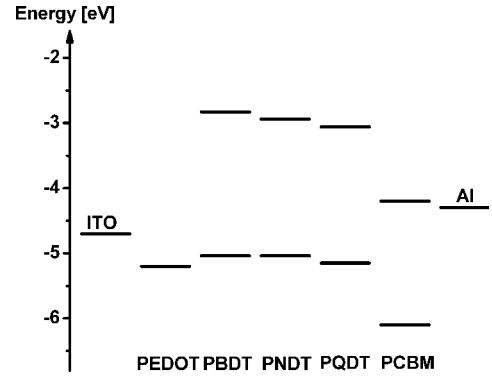

Figure 3. Energy diagram with HOMO/LUMO levels of **PBDT**, **PNDT**, **PQDT**, and PCBM in relation to the work functions of the electrode materials ITO/PEDOT:PSS and Al in a BHJ polymer/PCBM OPV device.

Photovoltaic Properties. PCBM as the electron-accepting component has been widely used in OPV devices. Figure 3 exhibits a diagram of energy levels of three alternating copolymers in relation to that of PCBM and the work functions of indium tin oxide (ITO), poly(3,4-ethylenedioxythiophene) poly(styrenesulfonate) (PEDOT:PSS), and aluminum (Al) used as electrodes in an OPV device. The LUMO energy levels of three copolymers are distinctively higher than that of PCBM. The difference between the LUMO energy levels of three copolymers and PCBM is over 1.2 eV, which is sufficiently high to enable an unrestricted and directed charge transfer.[28] Thus, all three copolymers were applied as donors into a conventional BHJ type OPV device with PCBM as acceptor in order to investigate the effect of different bridging π segments within the bithiophene moiety on the photovoltaic properties.

Hole mobility values for all copolymers were estimated via space-charge limit current (SCLC) by fabricating a hole-only device according to Blom's device configuration,[29,30] as detailed in the Experimental Section. The hole mobilities were found to be 3.01×10^{-5}, 1.3×10^{-5}, and 5.15×10^{-5} $cm^2\ V^{-1}\ s^{-1}$ for **PBDT**, **PNDT**, and **PQDT**, respectively.

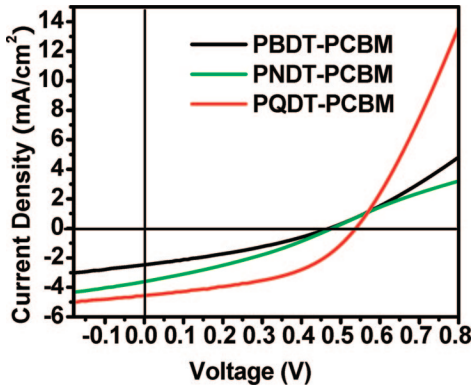

Figure 4. Typical $I-V$ characteristics (AM 1.5G, 100 mW/cm^2) of ITO/PEDOT:PSS(45 nm)/copolymer:PCBM (1:1.6, w/w)/Al(100 nm) devices.

Typical $I-V$ characteristics of ITO/PEDOT:PSS/copolymer:PCBM (1:1.6, w/w)/Al devices are depicted in Figure 4 under AM 1.5G irradiation (100 mW/cm^2). The devices with **PBDT**:PCBM layers (90 nm) showed an open-circuit voltage (V_{oc}) of 0.47 V, a short-circuit current density (J_{sc}) of 2.47 mA/cm^2, and a fill factor (*FF*) of 0.32, giving an energy conversion efficiency (η) of 0.38%. The V_{oc} value is close to the difference (0.82 V) between the HOMO energy level of **PBDT** and LUMO energy level of PCBM after the correction for an expected voltage loss of around 0.2 V at each electrode due to band bending.[31] The devices with **PNDT**:PCBM blends (90 nm) demonstrated a V_{oc} value of 0.47 V, a J_{sc} value of 3.61 mA/cm^2, and a *FF* of 0.33, leading to the η value of 0.55%, a slightly improved performance relative to **PBDT**. The same V_{oc} value of **PBDT** and **PNDT** based devices can be explained by the identical HOMO energy levels of both polymers (Table 2). Although the hole mobility of **PBDT** is slightly higher (3.01×10^{-5} cm^2 V^{-1} s^{-1}) than that of **PNDT** (1.3×10^{-5} cm^2 V^{-1} s^{-1}), the broader absorption of **PNDT** than that of **PBDT** resulted in higher short-circuit current and thus the slightly improved overall efficiency for **PNDT**-based devices. For the BHJ devices made from **PQDT**:PCBM films (100 nm), the devices exhibited an increased V_{oc} value of 0.53 V, also an increased J_{sc} value of 4.56 mA/cm^2, and an improved *FF* of 0.47, resulting in the significantly improved energy conversion efficiency of 1.14%. The increased V_{oc} value of **PQDT**-based devices is expected since **PQDT** has a lower HOMO energy level (−5.15 eV) than that of **PBDT** and **PNDT** (−5.04 eV). The increased current relative to that of **PNDT** is ascribed mainly to the fact that **PQDT** has higher hole mobility than that of **PNDT** since both polymers have the same band gap (2.10 eV). Tapping-mode atomic force microscopy (AFM) studies were carried out to investigate the film morphology of polymer:PCBM blends on their photovoltaic performances. Rough surfaces and blend phase separation were observed for **PBDT**:PCBM and **PNDT**:PCBM films (Supporting Information) compared to relatively smooth surface and more intimate mixing for **PQDT**:PCBM layer, which somehow explained better hole mobility of **PQDT** in devices over **PBDT** and **PNDT**. The improved miscibility of **PQDT** and PCBM, together with the higher V_{oc} value and smaller band gap, leads to the improved overall energy conversion efficiency.

The incident-photon-to-current efficiency (IPCE) spectra of the photovoltaic devices from copolymer:PCBM blends are presented in Figure 5 together with the absorption of thin films from copolymer:PCBM blends. The IPCE spectra of **PBDT** and **PNDT** match the optical absorptions well and show the maximum of 15% at 538 nm for **PBDT** and 27% at 555 nm for **PNDT**. For **PBDT**, a broad plateau around the maximum in IPCE spectrum exists between 500 and 580 nm, while occurring between 480 and 620 nm for **PNDT**. This phenomenon was caused by the stronger and wider absorption of **PNDT**:PCBM blend between 450 and 700 nm than that for **PBDT**:PCBM at the same film thickness. A similar match is found between the absorption spectrum and the IPCE spectrum for **PQDT**:PCBM films. The IPCE spectrum shows a maximum of 37% at 460 nm and an average value of 33% in the absorption area from 430 to 620 nm for devices based on **PQDT**:PCBM films. The higher IPCE value over the entire absorption wavelength region further explained the improved photovoltaic performance of **PQDT**:PCBM over the blends of the other two copolymers with PCBM.

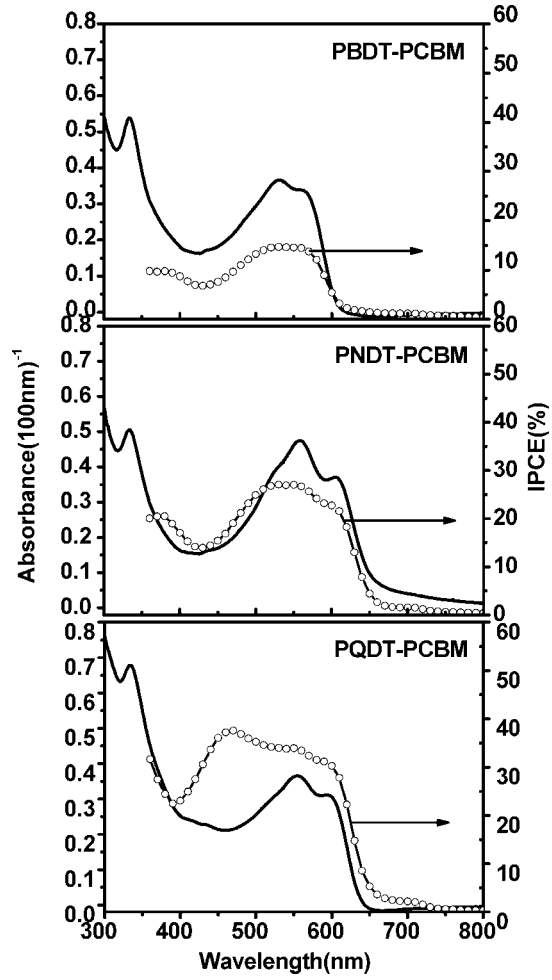

Figure 5. IPCE spectra (gray circled line) of BHJ photovoltaic devices ITO/PEDOT:PSS (45 nm)/copolymer:PCBM (1:1.6, w/w)/Al (100 nm) and the optical absorptions for the corresponding films of the blend from polymers and PCBM (black solid line) with the thickness of 100 nm.

Conclusions

We have successfully synthesized three alternating copolymers based on 4*H*-cyclopenta[2,1-*b*:3,4-*b*′]dithiophene as the common unit, while employing different structurally related conjugated units, namely, benzo[2,1-*b*:3,4-*b*′]dithiophene (**PBDT**), naphtho[2,1-*b*:3,4-*b*′]dithiophene (**PNDT**), and quinoxalino[2,1-*b*:3,4-*b*′]dithiophene (**PQDT**). By bridging intrinsically different π system to bithophene moiety to obtain enhanced π-electron delocalization and incorporating them into semiconductive alternating copolymers, the band gap as well as the HOMO and LUMO energy levels of resulting copolymers can be fine-tuned as demonstrated from the investigation of optical absorption properties and electrochemical studies of **PBDT**,

PNDT, and **PQDT**. The three copolymers were applied as electron-donating materials with PCBM as acceptor in conventional BHJ photovoltaic devices. A peak IPCE value of 37% and an overall power conversion efficiency of 1.14% were obtained from a **PQDT**/PCBM blend device, which is very encouraging given the quite large band gap of 2.1 eV for **PQDT**. Although the energy conversion efficiencies for these unoptimized photovoltaic devices are still not sufficiently high, this study enriched our understanding of tuning the electronic properties of conjugated semiconductive polymers for photovoltaic applications and provided further insights for future materials design.

Experimental Section

Reagents and Instrumentation. All reagents and chemicals were purchased from commercial sources (Aldrich, Acros, Strem, Fluka) and used without further purification unless stated otherwise. Reagent grade solvents were dried when necessary and purified by distillation. Melting points were uncorrected. Elemental analysis was carried out at the Atlantic Microlab. Gel permeation chromatography (GPC) measurements were performed on a Waters 2695 Separations Module apparatus with a differential refractive index detector with tetrahydrofuran (THF) as eluent. The obtained molecular weight is relative to the polystyrene standard. Thermogravimetric analysis (TGA) measurements were carried out with a Perkin-Elmer thermogravimetric analyzer (Pyris 1 TGA) at a heating rate of 10 °C min^{-1} under a nitrogen atmosphere. The temperature of degradation (T_d) is correlated to a 5% weight loss. Differential scanning calorimetry (DSC) analyses were recorded on a DSC220C instrument from Seiko Instruments. ^{1}H nuclear magnetic resonance (NMR) measurements were recorded with either a Bruker Avance 300 MHz AMX or a Bruker 400 MHz DRX spectrometer. ^{13}C nuclear magnetic resonance (NMR) measurements were carried out with a Bruker 400 MHz DRX spectrometer. Chemical shifts were expressed in parts per million (ppm), and splitting patterns are designated as s (singlet), d (doublet), t (triplet), and m (multiplet). Coupling constants J are reported in hertz (Hz). The mass spectroscopy was carried out on a Micromass Quattro II triple quadrupole mass spectrometer. 3,3′-Diiodo-2,2′-bithiophene,[22] 4,4-dioctyl-4*H*-cyclopenta[2,1-*b*:3,4-*b*′]dithiophene,[32] and benzo[2,1-*b*:3,4-*b*′]bithiophene-4,5-quinone (**5**)[33,34] were synthesized according to literature procedures.

Electrochemistry. Cyclic voltammetry measurements were carried out using a Bioanalytical Systems (BAS) Epsilon potentiostat equipped with a standard three-electrode configuration. Typically, a three-electrode cell equipped with a glassy carbon working electrode, a Ag/$AgNO_3$ (0.01 M in anhydrous acetonitrile) reference electrode, and a Pt wire counter electrode was employed. The measurements were done in anhydrous acetonitrile with tetrabutylammonium hexafluorophosphate (0.1 M) as the supporting electrolyte under an argon atmosphere at a scan rate of 100 mV/s. Polymer films were drop-cast onto the glassy carbon working electrode from a 2.5 mg/mL chloroform solution and dried under house nitrogen stream prior to measurements. The potential of Ag/$AgNO_3$ reference electrode was internally calibrated by using the ferrocene/ferrocenium redox couple (Fc/Fc^+). The electrochemical onsets were determined at the position where the current starts to differ from the baseline.

Spectroscopy. UV−vis absorption spectra were obtained by a Shimadzu UV-2401PC spectrophotometer. Fluorescence spectra were recorded on a Shimadzu RF-5301PC spectrofluorophotometer. For the measurements of thin films, polymers were spin-coated onto precleaned glass slides from 10 mg/mL polymer solutions in chlorobenzene.

AFM. Tapping mode with a Nanoscope III AFM (Digital Instruments, Inc., Santa Barbara, CA). The measurements were performed at ambient conditions (in air, 20 °C) using Si cantilevers with a spring constant of −50 N/m, a tip radius of 8 nm, and a resonance frequency of about 300 kHz.

Polymer Solar Cell Fabrication and Testing. Glass substrates coated with patterned indium-doped tin oxide (ITO) were purchased from Thin Film Devices, Inc. The 150 nm sputtered ITO pattern had a resistivity of 15 Ω/□. Prior to use, the substrates were ultrasonicated for 10 min in deionized water followed by the rinse with deionized water and the treatment in acetone and then 2-propanol in the same way. The substrates were dried under a stream of nitrogen and subjected to the treatment of UV-ozone over 20 min. A filtered dispersion of PEDOT:PSS in water (Baytron-PH500) was then spin-coated onto clean ITO substrates under 4000 rpm for 60 s and then baked at 130 °C for 15 min to give a thin film with a thickness of 45 nm. A blend of polymer and PCBM (1:1.6 w/w, 10 mg/mL for polymers) was dissolved in chlorobenzene with heating at 60 °C for 2 h, filtered through a 0.45 μm poly(tetrafluoroethylene) (PTFE) filter, and spin-coated at 1200 rpm for 60 s onto the PEDOT:PSS layer. The substrates were then dried under vacuum at room temperature for 12 h. The thicknesses of films were recorded by a profilometer (Alpha-Step 200, Tencor Instruments). The devices were finished for measurement after thermal deposition of 100 nm aluminum film as the cathode at a pressure of $\sim 1 \times 10^{-6}$ mbar. There are eight devices per substrate, with an active area of 18 mm^2 per device. Device characterization was carried out under AM 1.5G irradiation with the intensity of 100 mW/m^2 (Oriel 91160, 300 W) calibrated by a NREL certified standard silicon cell. Current vs potential ($I-V$) curves were recorded with a Keithley 2400 digital source meter. IPCE were detected under monochromatic illumination (Oriel Cornerstone 260 1/4 m monochromator equipped with an Oriel 70613NS QTH lamp), and the calibration of the incident light was performed with a monocrystalline silicon diode. All fabrication steps after adding the PEDOT:PSS layer onto ITO substrate, and characterizations were performed in gloveboxes under a nitrogen atmosphere. For mobility measurements, the hole-only devices in a configuration of ITO/PEDOT:PSS (45 nm)/copolymer−PCBM (1:1.6, w/w)/Pd (40 nm) were fabricated. The experimental dark current densities J of polymer:PCBM blends were measured when applied with voltage from 0 to 6 V. The applied voltage V was corrected from the built-in voltage V_{bi},[30] which was taken as a compensation voltage $V_{bi} = V_{oc} + 0.05$ V and the voltage drop V_{rs} across the indium tin oxide/poly(3,4-ethylenedioxythiophene):poly(styrenesulfonic acid) (ITO/PEDOT:PSS) series resistance and contact resistance, which is found to be around 35 Ω from a reference device without the polymer layer. From the plots of $J^{0.5}$ vs V (Supporting Information), hole mobilities of copolymers can be deduced from[35]

$$J = \frac{9}{8}\varepsilon_r\varepsilon_0\mu_h\frac{V^2}{L^3} \tag{4}$$

where ε_0 is the permittivity of free space, ε_r is the dielectric constant of the polymer which is assumed to be around 3 for the conjugated polymers in our experiment,[36] μ_h is the hole mobility, V is the voltage drop across the device, and L is the film thickness of active layer.

Synthesis. (6*S*,11*S*)-9-hydroxy-2,6,11,15-tetramethylhexadeca-2,14-dien-8-one (1). [37] To a 250 mL of two-necked round-botton (RB) flask containing (−)citronellal (25.0 g, 163 mmol) in 50 mL of ethanol under argon was added the catalyst of 3-ethyl-5-(2-hydroxyethyl)-4-methylthiazolium bromide (4.1 g, 16.3 mmol) and triethylamine (17.0 mL, 120 mmol). The mixture was then heated to reflux overnight. After removal of the solvent under reduced pressure, the resulted mixture was poured into 100 mL of water and extracted by ethyl ether (3 × 60 mL). The combined organic layer was dried over anhydrous $MgSO_4$ and concentrated under vacuum. The residue was purified by flash chromatography on silica gel (hexane:ethyl acetate = 20:1, v/v) to afford 18.5 g of product as a colorless oil (yield: 75%). ^{1}H NMR (400 MHz, $CDCl_3$): δ 5.08 (m, 2H), 4.15 (m, 1H), 3.47 (dd, 1H, J = 5.04 Hz), 2.40 (m, 1H), 2.2 (m, 1H), 1.9−2.1 (m, 6H), 1.60 (d, 12H), 1.1−1.3 (m, 4H), 0.8−1.0 (m, 6H). ^{13}C NMR (400 MHz, $CDCl_3$): δ 212.63, 131.63, 131.30, 124.52, 124.40, 124.00, 75.59, 74.70, 45.16, 45.15,

41.15, 41.00, 37.95, 36.85, 36.83, 35.56, 29.36, 29.04, 28.92, 28.81, 25.65, 25.42, 25.39, 25.36, 25.22, 20.29, 19.82, 19.65, 18.46, 17.60.

(6*S*,11*S*)-2,6,11,15-tetramethylhexadeca-2,14-diene-8,9-dione (2). To a solution of **1** (7.0 g, 22.7 mmol) in 100 mL of methylene chloride was added 7.5 g of PCC. The mixture was heated to reflux. After 16 h, the mixture was cooled to room temperature and filtered. The solution was concentrated under reduced pressure. The crude compound was purified by flash chromatography on silica gel (hexane:ethyl acetate = 20:1, v/v) to afford the product as a colorless oil. Yield: 3.5 g (50%). ^{1}H NMR (400 MHz, $CDCl_3$): δ 5.06 (m, 2H), 2.66−2.74 (dd, 2H, J = 5.64, 16.71 Hz), 2.51−2.60 (dd, 2H, J = 7.98, 16.73 Hz), 1.92−2.02 (m, 6H), 1.5−1.67 (s, 6H), 1.58 (s, 6H), 1.19−1.35 (m, 4H), 0.89 (d, 6H, J = 6.66 Hz). ^{13}C NMR (400 MHz, $CDCl_3$): δ 200.05, 131.60, 124.07, 52.96, 36.94, 28.49, 25.66, 25.36, 19.71, 17.60.

(6S,11S)-2,6,11,15-tetramethylhexadeca-2,14-diene-8,9-dione dioxime (3). A 250 mL of two-necked RB flask containing a solution of **2** (6.12 g, 20.0 mmol) in ethanol (60 mL) and pyridine (8.0 mL) was purged with argon. Hydroxyammonium chloride (7.0 g, 100.0 mmol) was then added in one portion. The mixture was heated to reflux for 5 h. After removal of the solvent under reduced pressure, 100 mL of water/ethanol (2:1, v/v) was added and ultrasonicated before filtration. The solid was then rinsed by 20 mL of cold methanol and dried under vacuum to afford a white pure solid. Yield: 5.5 g (95%); mp 131−131.6 °C. ^{1}H NMR (400 MHz, CD_3OD): δ 4.93 (m, 2H), 3.16 (m, 2H), 2.32−2.47 (m, 4H), 1.72−1.90 (m, 6H), 1.51 (s, 6H), 1.44 (s, 6H), 1.17−1.20 (m, 2H), 1.01−1.05 (m, 2H), 0.72 (d, 6H, J = 6.7 Hz). ^{13}C NMR (400 MHz, CD_3OD): δ 157.95, 131.66, 126.05, 38.51, 32.19, 31.42, 26.68, 25.86, 20.16, 17.68.

(6S,11S)-2,6,11,15-tetramethylhexadecane-8,9-diamine dihydrogen chloride (4). To a solution of **3** (1.9 g) in 50 mL of absolute ethanol at room temperature was added platinum oxide (0.4 g) and 2.0 mL of concentrated hydrogen chloride. The mixture was then purged with hydrogen and was kept stirring under hydrogen (with a hydrogen balloon) over 10 h. After removing the solvent under reduced pressure, the residue was rinsed with cold hexane and directly used in the next step without further purification.

2,3-Bis((S)-2,6-dimethylheptyl)dithieno[3,2-f:2′,3′-h]quinoxaline (6). To a 100 mL of two-necked RB flask equipped with a condenser was added the solution of **4** (1.20 g) in 50 mL of methanol, **5** (0.66 g, 3 mmol) and 2.0 mL of pyridine. The mixture was then heated to reflux with stirring overnight. After removing the solvent under reduced pressure, the residue was redissolved in 30 mL of methylene chloride and washed by water and dried over anhydrous $MgSO_4$. The organic layer was then concentrated, and the residue was purified by flash chromatography on silica gel (hexane:methylene chloride = 4:1, v/v) to afford 0.91 g of pure product as a white solid (yield 60%); mp 57.5−58.7 °C. ^{1}H NMR (300 MHz, $CDCl_3$): δ 8.31 (d, 2H, J = 5.28 Hz), 7.51 (d, 2H, J = 5.22 Hz), 2.94−3.16 (dd, 2H, J = 6.08 Hz, 14.2 Hz), 2.87−2.90 (dd, 2H, J = 8.0 Hz, 14.2 Hz), 2.33 (m, 2H), 1.55 (m, 2H), 1.2−1.52 (m, 12H), 1.03 (d, 6H, J = 6.58 Hz). 0.88 (d, 12H, J = 7.45 Hz). ^{13}C NMR (400 MHz, $CDCl_3$): δ 154.06, 136.04, 135.11, 133.95, 124.12, 42.13, 39.23, 37.36, 32.91, 27.98, 24.87, 22.71, 22.59, 19.82. MS: m/z = 496.6 $[M + 2H]^+$ (Calcd: 494.3).

6,9-Dibromo-2,3-bis((S)-2,6-dimethylheptyl)dithieno[3,2-f:2′,3′-h]quinoxaline (7). To a solution of **6** (0.99 g, 2.0 mmol) in 20 mL of chloroform/acetic acid (1:1, v/v) at room temperature was added NBS (0.75 g, 4.2 mmol). The resulting mixture was stirred at room temperature for 24 h and then diluted by 50 mL of water. The organic layer was washed by 5% sodium hydroxide solution, water, and brine and dried over anhydrous $MgSO_4$. After removing the solvent, the crude product was further purified by flash chromatography on silica gel (hexane:methylene chloride = 5:1, v/v) to afford 0.85 g of pure product as a white solid (yield 65%); mp 106.4−107.9 °C. ^{1}H NMR (300 MHz, $CDCl_3$): δ 8.15 (s, 2H), 3.00−3.07 (dd, 2H, J = 6.05 Hz, 14.38 Hz), 2.78−2.85 (dd, 2H, J = 7.96 Hz, 14.38 Hz), 2.28 (m, 2H), 1.55 (m, 2H), 1.17−1.45 (m, 12H), 0.98 (d, 6H, J = 6.60 Hz). 0.88 (d, 12H, J = 6.58 Hz). ^{13}C NMR (400 MHz, $CDCl_3$): δ 155.12, 135.13, 134.73, 133.60, 126.73, 112.97, 42.17, 39.27, 37.39, 32.73, 28.03, 24.88, 22.73, 22.61, 19.86. MS: m/z = 652.6 $[M + 2H]^+$ (Calcd: 650.1). Anal. Calcd for $C_{30}H_{40}Br_2N_2S_2$: C, 55.21; H, 6.18; Br, 24.49; N, 4.29; S, 9.83. Found: C, 55.49; H, 6.24; Br, 24.59; N, 4.18; S, 9.78.

2,6-Bis(4,4,5,5-tetramethyl-1,3,2-dioxaborolan-2-yl)-4,4-dioctyl-4H-cyclopenta[2,1-b:3,4-b′]dithiophene (8). A solution of 4,4-dioctyl-4*H*-cyclopenta[2,1-*b*:3,4-*b*′]dithiophene (1.2 g, 3.0 mmol) in 20 mL of dry THF under argon was cooled to −78 °C, and *n*-BuLi in hexane (2.5 M, 4.8 mL, 12 mmol) was added over 10 min with stirring. The mixture was kept at −78 °C for another 1 h before 2-isopropoxy-4,4,5,5-tetramethyl[1,3,2]dioxaborolane (3.2 mL, 25 mmol) was added. The cooling bath was removed after 3 h, and the mixture was allowed to warm to room temperature overnight (16 h). After subsequent dilution with ethyl ether and washing with brine and large amount of water, the organic layer was dried over anhydrous $MgSO_4$ and concentrated under reduced pressure to give a solid which was washed further with cold methanol and dried in vacuo to afford the pure product as a pale yellow solid (1.4 g, 71%); mp 109−110 °C. ^{1}H NMR (300 MHz, $CDCl_3$): δ 7.42 (s, 2H), 1.79 (m, 4H), 1.36 (s, 24H), 1.1−1.24 (m, 10H), 0.90−0.93 (m, 4H), 0.84 (t, 6H, J = 7.08 Hz). ^{13}C NMR (400 MHz, $CDCl_3$): δ 161.41, 143.84, 131.04, 83.97, 52.74, 37.79, 31.75, 29.99, 29.24, 24.76, 24.46, 22.56, 14.02. MS: m/z = 654.6 $[M]^+$ (Calcd: 654.4). Anal. Calcd for $C_{37}H_{60}B_2O_4S_2$: C, 67.89; H, 9.24; S, 9.80. Found: C, 68.05; H, 9.41; S, 9.72.

4,5-Dioctylbenzo[2,1-b:3,4-b′]dithiophene. [23] To a two-necked RB flask under nitrogen was added 1.39 g (3.3 mmol) of 3,3′-diiodo-2,2′-bithiophene, 222 mg (0.33 mmol) of $Pd(OAc)_2$, 2.5 g (10 mmol) of 9-octadecyne, 1.85 g (10 mmol) of tributylamine, and 10 mL of anhydrous DMF. The mixture was heated at 130 °C for 4 h. After cooling down to room temperature, 50 mL of ether ethyl was added. The organic phase was washed with water several times, dried by $MgSO_4$, and concentrated under reduced pressure. The residue was further purified by flash chromatography on silica gel (hexane as eluent) to afford the pure product as a colorless liquid (1.16 g, yield: 85%). ^{1}H NMR (300 MHz, $CDCl_3$): δ 7.46 (d, 2H, J = 5.43 Hz), 7.37 (d, 2H, J = 5.42 Hz), 3.01 (t, 4H, J = 7.89 Hz), 1.68 (m, 4H), 1.51 (m, 4H), 1.30 (m, 16H), 0.89 (t, 6H, J = 6.7 Hz). ^{13}C NMR (400 MHz, $CDCl_3$): δ 137.47, 131.58, 131.32, 123.55, 123.38, 31.87, 31.52, 30.43, 30.16, 29.48, 29.27, 22.63, 14.04. MS: m/z = 414.7 $[M]^+$ (Calcd: 414.7).

2,7-Dibromo-4,5-dioctylbenzo[2,1-b:3,4-b′]dithiophene. To a solution of 4,5-dioctylbenzo[2,1-*b*:3,4-*b*′]dithiophene (0.83 g, 2 mmol) in 10 mL of chloroform/glacial acetic acid (1:1, v/v) was added 0.72 g of NBS at room temperature. After the reaction was completed, 20 mL of chloroform was added. The mixture was then washed by water, 5% NaOH, and brine. After drying with anhydrous $MgSO_4$, the organic phase was concentrated, and the residue was further purified by flash chromatography on silica gel (hexane as eluent) to give 0.8 g of final product (yield 70%); mp 63.8−65.2 °C. ^{1}H NMR (300 MHz, $CDCl_3$): δ 7.39 (s, 2H), 2.88 (t, 4H, J = 8.25 Hz), 1.58 (m, 4H), 1.48 (m, 4H), 1.32 (m, 16H), 0.89 (t, 6H, J = 6.9 Hz). ^{13}C NMR (400 MHz, $CDCl_3$): δ 137.28, 131.46, 131.40, 126.26, 112.53, 31.89, 31.41, 30.36, 30.10, 29.44, 29.28, 22.67, 14.08. MS: m/z = 572.6 $[M]^+$ (Calcd: 572.5). Anal. Calad. for $C_{26}H_{36}Br_2S_2$: C, 54.55; H, 6.34; Br, 27.91; S, 11.20. Found: C, 54.75; H, 6.32; Br, 27.89; S, 11.35.

1,2-Dioctylbenzene. The synthesis of 1,2-dioctylbenzene and 4,5-dioctyyl-1,2-diiodobenzene was adopted from the reported procedure.[38] A flame-dried, 250 mL three-necked RB flask equipped with a condenser and an addition funnel was loaded with magnesium metal turnings (12.0 g, 0.48 mol) in 20 mL of anhydrous ethyl ether under an argon atmosphere. A solution of 1-bromooctane (80.5 mL, 0.46 mol) in 50 mL of anhydrous ethyl ether was added dropwise in a rate that a gentle reflux was maintained. After the addition of the bromide solution, the resulting mixture was heated under reflux for an additional 2 h. After cooling to room temperature, the clear solution of the Grignard reagent was transferred through a cannula into a flame-dried addition funnel and added dropwise to a stirred solution of 1,2-dichlorobenzene (23 mL, 0.2

mol) and 1,3-bis(diphenylphosphino)propane)nickel(II) chloride (0.7 g, 1.29 mmol) in 50 mL of anhydrous ethyl ether at room temperature. The reaction mixture was then heated to reflux overnight and then cooled to room temperature and poured into 200 mL of hydrochloric acid (2 M) with ice. The organic layer was separated and washed with water, Na_2CO_3, brine, and water and dried over anhydrous $MgSO_4$. After removing the solvent under reduced pressure, the residue was purified by passing through a short silica gel column (hexane as eluent). The distillation of the resulting oil under reduced pressure gave 39.0 g of pure 1,2-dioctylbenzene (138 °C/0.25 mmHg) as a colorless liquid (yield 65%). ^{1}H NMR (400 MHz, $CDCl_3$): δ 7.12 (m, 4H), 2.59 (t, 4H, J = 7.76 Hz), 1.56 (m, 4H), 1.27−1.37 (m, 20H), 0.88 (t, 6H, J = 6.36 Hz). ^{13}C NMR (400 MHz, $CDCl_3$): δ 140.56, 129.08, 125.66, 32.69, 31.90, 31.35, 29.81, 29.51, 29.28, 22.68, 14.11. MS: m/z = 302.3 $[M]^+$ (Calcd: 302.3).

4,5-Dioctyl-1,2-diiodobenzene. 1,2-Dioctylbenzene (12.3 g, 40.6 mol) was added to a RB flask loaded with glacial acetic acid (150 mL), H_2SO_4 (concentrated, 9.0 mL), H_2O (1 mL), $NaIO_3$ (4.016 g, 20.3 mmol), and I_2 (11.34 g, 44.7 mmol) at room temperature. The resulting mixture was then heated under reflux overnight. After cooling to room temperature, a saturated aqueous $Na_2S_2O_4$ solution was added until the color of the mixture changed from purple to light brown. The mixture was then extracted with CH_2C1_2 (50 mL × 3), washed with saturated $Na_2S_2O_4$, H_2O, and brine, and then dried over anhydrous Na_2SO_4. After removing the solvent under reduced pressure, the brownish residue was purified by flash chromatography on silica gel to afford a colorless oil (18.7 g, yield 83%). ^{1}H NMR (400 MHz, $CDCl_3$): δ 7.60 (s, 2H), 2.46 (t, 4H, J = 8.0 Hz), 1.52 (m, 4H), 1.27−1.37 (m, 20H), 0.88 (t, 6H, J = 7.04 Hz). ^{13}C NMR (400 MHz, $CDCl_3$): δ 142.62, 139.69, 103.97, 31.87, 31.80, 30.85, 29.54, 29.35, 29.16, 22.60, 14.05. MS: m/z = 554.1 $[M]^+$ (Calcd: 554.1).

4,5-Bis(3-thienyl)-1,2-dioctylbenzene. [18] To a three-necked 250 mL RB flask equipped with a condenser was added 4,5-dioctyl-1,2-diiodobenzene (11.08 g, 20 mmol), 3-thiopheneboronic acid (6.4 g, 50.0 mmol), and Na_2CO_3 (24.0 g, 226 mmol) in a mixed solvent of toluene (50 mL), EtOH (50 mL), and H_2O (50 mL). The resulting mixture was vigorously stirred during the cycle of evacuation/refilling with argon three times. The catalyst $Pd(PPh_3)_4$ (1% equiv, 575 mg, 0.54 mmol) was then added to the mixture under a gentle argon stream, and the system was heated at reflux overnight. After cooling to room temperature, the reaction mixture was diluted with 100 mL of ethyl ether and the aqueous layer was removed. The organic layer was washed with water and brine and dried with anhydrous $MgSO_4$. After the solvent removal under reduced pressure, the residue was purified by flash chromatography on silica gel (hexane:ethyl acetate = 20:1, v/v) to provide 7.2 g of the product (yield 78%). ^{1}H NMR (400 MHz, $CDCl_3$): δ 7.25 (s, 2H), 7.17 (dd, 2H, J = 4.92 Hz, 2.98 Hz), 7.05 (dd, 2H, J = 1.22 Hz, 2.97 Hz), 6.80 (dd, 2H, J = 1.23 Hz, 4.94 Hz), 2.66 (t, 4H, J = 7.80 Hz), 1.65 (m, 4H), 1.30−1.50 (m, 20H), 0.90 (t, 6H, J = 6.96 Hz). ^{13}C NMR (400 MHz, $CDCl_3$): δ 142.20, 140.03, 132.65, 130.92, 129.08, 124.39, 122.38, 32.45, 31.91, 31.40, 29.88, 29.51, 29.29, 22.68, 14.13. MS: m/z = 466.3 $[M]^+$ (Calcd: 466.2).

5,6-Dioctylnaphtho[2,1-b:3,4-b′]dithiophene. In a quartz tube was added a solution of 4,5-bis(3-thienyl)-1,2-dioctylbenzene (0.5 g, 1.1 mmol) and iodine (30 mg) in toluene (500 mL). The system was then irradiated by a 400 W mercury lamp equipped with an efficient cooling system for 16 h under magnetic stirring and air bubbling. The reaction mixture was washed with a saturated aqueous solution of $Na_2S_2O_3$, dried over $MgSO_4$, and concentrated. The residue was purified by flash chromatography on silica gel (hexane as eluent), and a white solid was obtained (0.33 g, yield 65%); mp 62.2−63.1 °C. ^{1}H NMR (400 MHz, $CDCl_3$): δ 8.11 (s, 2H), 7.97 (d, 2H, J = 5.34 Hz), 7.47 (d, 2H, J = 5.30), 2.86 (t, 4H, J = 7.76 Hz), 1.74 (m, 4H), 1.32−1.50 (m, 20H), 0.92 (t, 6H, J = 6.80 Hz). ^{13}C NMR (400 MHz, $CDCl_3$): δ 139.22, 134.12, 131.25, 126.09, 124.04, 123.34, 122.74, 33.14, 31.29, 31.52, 29.86, 29.58, 29.34, 22.70, 14.14. MS: m/z = 464.4 $[M]^+$ (Calcd: 464.2).

2,9-Dibromo-5,6-dioctylnaphtho[2,1-b:3,4-b′]dithiophene. To a stirred solution of 5,6-dioctylnaphtho[2,1-*b*:3,4-*b*′]dithiophene (1 g, 2.16 mmol) in a mixture of chloroform−acetic acid (1/1, v/v, 10 mL) at room temperature was added NBS (0.773 g, 4.3 mmol). The resulting solution was stirred overnight. The mixture was poured into 100 mL of water and extracted with chloroform (50 mL). The combined organic layer was further washed with 5% aqueous NaOH solution, brine, and water, dried with $MgSO_4$, and concentrated under reduced pressure. The residue was purified by flash chromatography on silica gel to give 0.92 g of the pure product (yield 68%); mp 105.3−106.4 °C. ^{1}H NMR (400 MHz, $CDCl_3$): δ 7.84 (s, 2H), 7.80 (d, 2H), 2.79 (m, 4H, J = 7.63 Hz), 1.70 (m, 4H), 1.31−1.48 (m, 20H), 0.91 (t, 6H, J = 6.91 Hz). ^{13}C NMR (400 MHz, $CDCl_3$): δ 139.84, 133.84, 130.90, 125.51, 124.90, 123.64, 111.98, 33.08, 31.93, 31.31, 29.88, 29.57, 29.35, 22.71, 14.14. MS: m/z = 620.2 $[M]^+$ (Calcd: 620.0). Anal. Calcd for $C_{30}H_{38}Br_2S_2$: C, 57.88; H, 6.15; Br, 25.67; S, 10.30. Found: C, 57.97; H, 6.20; Br, 25.84; S, 10.38.

Synthesis of Alternating Copolymers via Suzuki Coupling Polymerization. A representative procedure is as follows. To a flame-dried 25 mL two-necked RB flask equipped with a condenser was added **7** (195.8 mg, 0.3 mmol), **8** (196.4 mg, 0.3 mmol), 6.0 mL of 2 M Na_2CO_3, 10 mL of toluene, and 2 drops of Aliquat 336 under a gentle argon stream with vigorous stirring. The resulting mixture was evacuated and refilled with argon for three cycles to remove oxygen and then was added $Pd(PPh_3)_4$ (17 mg, 0.015 mmol, 5% equiv) under an argon stream. The mixture was heated under reflux over 7 days. After cooling to room temperature, the organic layer was separated and washed by water. Addition of 100 mL of methanol to organic solution offered the precipitate, which was collected by filtration and successively washed with water and methanol and dried under air. The crude polymer was then extracted subsequently with methanol, acetone, and chloroform in a Soxhlet extractor. The fraction from chloroform was concentrated under reduced pressure and precipitated into methanol to give the polymer **PQDT** as a blue solid (0.23 g, 86%). ^{1}H NMR (400 MHz, $CDCl_3$): δ 7.79 (2H), 7.32 (2H), 3.08 (2H), 2.86 (2H), 2.32 (2H), 1.98 (4H), 1.20−1.80 (H), 0.95 (6H), 0.85 (6H).

PBDT yield: 0.23 g (88%). ^{1}H NMR (400 MHz, $CDCl_3$): δ 7.46 (2H), 7.17 (2H), 2.98 (4H), 1.92(4H), 1.80−1.22 (48H), 0.93 (6H), 0.85 (6H).

PNDT yield: 0.22 g (90%). ^{1}H NMR (400 MHz, $CDCl_3$): δ 7.97 (2H), 7.85 (2H), 7.38 (2H), 2.85 (4H), 2.01 (4H), 1.9−1.2 (48H), 0.98−0.7 (12H).

Acknowledgment. This work was supported by the University of North Carolina at Chapel Hill and the National Science Foundation STC Program at UNC Chapel Hill (CHE-9876674). We thank Mr. Peng Dai for acquiring AFM images and Dr. Paul G. Hoertz for helpful discussions.

Supporting Information Available: TGA data, ^{1}H spectra, fluorescence spectra, cyclic voltammograms of three copolymers; $I-V$ characteristics of the blend of **PQDT**/PCBM film in different mass ratio and film thickness, AFM image of polymer:PCBM blends, and $J^{0.5}$ vs V plots of mobility measurement of three copolymers. This material is available free of charge via the Internet at http://pubs.acs.org.

References and Notes

(1) Ma, W. L.; Yang, C. Y.; Gong, X.; Lee, K.; Heeger, A. J. *Adv. Funct. Mater.* **2005**, *15*, 1617–1622.
(2) Li, G.; Shrotriya, V.; Huang, J. S.; Yao, Y.; Moriarty, T.; Emery, K.; Yang, Y. *Nat. Mater.* **2005**, *4*, 864–868.
(3) Thompson, B. C.; Fréchet, J. M. J. *Angew. Chem., Int. Ed.* **2008**, *47*, 58–77.
(4) Scharber, M. C.; Wuhlbacher, D.; Koppe, M.; Denk, P.; Waldauf, C.; Heeger, A. J.; Brabec, C. L. *Adv. Mater.* **2006**, *18*, 789–794.
(5) Brabec, C. J.; Winder, C.; Sariciftci, N. S.; Hummelen, J. C.; Dhanabalan, A.; van Hal, P. A.; Janssen, R. A. J. *Adv. Funct. Mater.* **2002**, *12*, 709–712.

(6) Muhlbacher, D.; Scharber, M.; Morana, M.; Zhu, Z. G.; Waller, D.; Gaudiana, R.; Brabec, C. *Adv. Mater.* **2006**, *18*, 2884–2889.
(7) Peet, J.; Kim, J. Y.; Coates, N. E.; Ma, W. L.; Moses, D.; Heeger, A. J.; Bazan, G. C. *Nat. Mater.* **2007**, *6*, 497–500.
(8) Zhang, F. L.; Jespersen, K. G.; Bjorstrom, C.; Svensson, M.; Andersson, M. R.; Sundstrom, V.; Magnusson, K.; Moons, E.; Yartsev, A.; Inganas, O. *Adv. Funct. Mater.* **2006**, *16*, 667–674.
(9) Andersson, L. M.; Zhang, F. L.; Inganas, O. *Appl. Phys. Lett.* **2007**, *91*, 071108/1–071108/3.
(10) Slooff, L. H.; Veenstra, S. C.; Kroon, J. M.; Moet, D. J. D.; Sweelssen, J.; Koetse, M. M. *Appl. Phys. Lett.* **2007**, *90*, 143506/1–143506/3.
(11) Wienk, M. M.; Turbiez, M. G. R.; Struijk, M. P.; Fonrodona, M.; Janssen, R. A. J. *Appl. Phys. Lett.* **2006**, *88*, 153511/1–153511/3.
(12) Yao, Y.; Shi, C. J.; Li, G.; Shrotriya, V.; Pei, Q. B.; Yang, Y. *Appl. Phys. Lett.* **2006**, *89*, 153507/1–153507/3.
(13) Ashraf, R. S.; Shahid, M.; Klemm, E.; Al-Ibrahim, M.; Sensfuss, S. *Macromol. Rapid Commun.* **2006**, *27*, 1454–1459.
(14) Blouin, N.; Michaud, A.; Leclerc, M. *Adv. Mater.* **2007**, *19*, 2295–2300.
(15) Blouin, N.; Michaud, A.; Gendron, D.; Wakim, S.; Blair, E.; Neagu-Plesu, R.; Belletete, M.; Durocher, G.; Tao, Y.; Leclerc, M. *J. Am. Chem. Soc.* **2008**, *130*, 732–742.
(16) Roncali, J. *Chem. Rev.* **1997**, *97*, 173–205.
(17) Tovar, J. D.; Rose, A.; Swager, T. M. *J. Am. Chem. Soc.* **2002**, *124*, 7762–7769.
(18) Tovar, J. D.; Swager, T. M. *Adv. Mater.* **2001**, *13*, 1775–1780.
(19) *Polycyclic Hydrocarbons I and II*; Clar, E., Ed.; Academic Press: London, 1964.
(20) Watson, M. D.; Fechtenkotter, A.; Müllen, K. *Chem. Rev.* **2001**, *101*, 1267–1300.
(21) Shklyarevskiy, I. O.; Jonkheijm, P.; Stutzmann, N.; Wasserberg, D.; Wondergem, H. J.; Christianen, P. C. M.; Schenning, A.; de Leeuw, D. M.; Tomovic, Z.; Wu, J. S.; Müllen, K.; Maan, J. C. *J. Am. Chem. Soc.* **2005**, *127*, 16233–16237.
(22) Miura, M.; Satoh, T.; Watanabe, H.; Ueda, M. WO/2007/105638, **2007**.
(23) Watanabe, H.; Kumagai, J.; Tsurugi, H.; Satoh, T.; Miura, M. *Chem. Lett.* **2007***36*, 1336–1337.
(24) Jayasuriya, N.; Kagan, J.; Owens, J. E.; Kornak, E. P.; Perrine, D. M. *J. Org. Chem.* **1989**, *54*, 4203–4205.
(25) Nicolas, Y.; Blanchard, P.; Levillain, E.; Allain, M.; Mercier, N.; Roncali, J. *Org. Lett.* **2004**, *6*, 273–276.
(26) Pommerehne, J.; Vestweber, H.; Guss, W.; Mahrt, R. F.; Bassler, H.; Porsch, M.; Daub, J. *Adv. Mater.* **1995**, *7*, 551–554.
(27) Zhan, X. W.; Liu, Y. Q.; Wu, X.; Wang, S. A.; Zhu, D. B. *Macromolecules* **2002**, *35*, 2529–2537.
(28) Arkhipov, V. I.; Bassler, H. *Phys. Status Solidi A* **2004**, *201*, 1152–1187.
(29) Melzer, C.; Koop, E. J.; Mihailetchi, V. D.; Blom, P. W. M. *Adv. Funct. Mater.* **2004**, *14*, 865–870.
(30) Mihailetchi, V. D.; Koster, L. J. A.; Blom, P. W. M.; Melzer, C.; de Boer, B.; van Duren, J. K. J.; Janssen, R. A. J. *Adv. Funct. Mater.* **2005**, *15*, 795–801.
(31) Mihailetchi, V. D.; Blom, P. W. M.; Hummelen, J. C.; Rispens, M. T. *J. Appl. Phys.* **2003**, *94*, 6849–6854.
(32) Coppo, P.; Cupertino, D. C.; Yeates, S. G.; Turner, M. L. *J. Mater. Chem.* **2002**, *12*, 2597–2599.
(33) Wynberg, H.; Sinnige, H. J. M. *Recl. Trav. Chim.* **1969**, *88*, 1244–1245.
(34) Ohnishi, H.; Kozaki, M.; Okada, K. *Synth. Met.* **2003**, *135*, 85–86.
(35) Goodman, A. M.; Rose, A. *J. Appl. Phys.* **1971**, *42*, 2823–2830.
(36) Goh, C.; Kline, R. J.; McGehee, M. D.; Kadnikova, E. N.; Fréchet, J. M. J. *Appl. Phys. Lett.* **2005**, *86*, 122110–122113.
(37) Popp, F. D. *J. Heterocycl. Chem.* **1974**, *11*, 79–82.
(38) Zhou, Q.; Carroll, P. J.; Swager, T. M. *J. Org. Chem.* **1994**, *59*, 1294–1301.

MA800776Q